



## 3D HYBRID SIMULATION OF THE SOURCE AND SITE EFFECTS DURING THE 1999 ATHENS EARTHQUAKE

Ivo OPRŠAL<sup>1,2</sup>, Jiří ZAHRADNÍK<sup>2</sup>, Anna SERPETSIDAKI<sup>3</sup> and G-Akis TSELENTIS<sup>3</sup>

### SUMMARY

Combined source-path-site effects due to the  $M_w=5.9$  1999 Athens Earthquake are computed via efficient hybrid method. The method couples finite-extent source kinematic modeling, and 1D discrete-wavenumber crustal propagation with 3D finite-difference method for the local site effects, thus saving considerably computer memory and time. Simulation up to 6Hz proves that the intensities of IX at the Ano Liosia suburban area was due to proximity and directivity of the source, as well as due to complex 3D site effects. The simulated ground acceleration locally exceeds 0.6 g, and the response spectra indicate major effects at 2-4 Hz.

### INTRODUCTION

The damaging 1999 Athens earthquake of  $M_w=5.9$  occurred at about 20 km from the city center. The intensity distribution in the capital, ranging from V to IX, was quite irregular due to combination of the source, path and site effects. The 30-stations temporary network, installed in Athens by the University of Patras, recorded and located more than 400 aftershocks. The horizontal-to-vertical spectral ratios from the 20 selected aftershock recordings provided site classification. The most significant anomaly ( $H/V$  exceeding 4 in the frequency range 1-4 Hz) was found at the Ano Liosia site, belonging to the most heavily damaged zones with intensity IX. The site is situated in a shallow basin whose surface extent is about 4 km x 4 km, and the maximum depth is of about 150 m. The basin is filled with basically 3 layers. The topmost layer includes alluvium and soft soil, the second one consists of stiff soil and alternations of conglomerates, clay and sand, while the third layer is represented by Neogene formations like marl, marly limestone and sandstone. The bedrock of the basin consists of Triassic limestone and schist. Borders of the basin, where the topmost layer directly overlies the bedrock, are locally quite steep. Based on geophysical data ( $V_p$ ,  $V_s$ ,  $Q$ ) measured at the site, the numerical modeling of the seismic site response was carried out. The 3D finite-difference technique was used, and significant effects were revealed. No recording of the mainshock is available in Ano Liosia. Nevertheless, based on the finite-extent composite source model, validated in central Athens by the existing strong motion records of the mainshock, we found that the bedrock motion in Ano Liosia had its PGA ranging from 0.2 to 0.3 g, resulting from the relatively small epicentral distance ( $\sim 10$  km) and the forward source directivity. The source and site

---

<sup>1</sup> Swiss Seismological Service, ETH Zurich, Switzerland

<sup>2</sup> Faculty of Mathematics and Physics, Charles University in Prague, Czech Republic

<sup>3</sup> Seismological Laboratory, University of Patras, Greece

effects were combined with each other by a hybrid technique, allowing fast full-wave 3D calculations up to ~6 Hz on a standard personal computer, and showing that the combined source and site effects in Ano Liosia have provided the PGA values locally exceeding 0.6 g.

## THE HYBRID METHOD

The hybrid method is based on a specific 3D approach (Opršal and Zahradník [1]) where the source, path, and site effects are computed in two successive steps. The first step (source and path) is realized by any 3D method (e.g., discrete wavenumber (DWN), ray, finite differences (FD)). The particle motion from this modeling (so called excitation) is saved on a set of receivers covering a formal excitation box comprising the local site of interest. At this stage, there is no local structure present in this box. The second step of the hybrid method is performed by FD on an irregular rectangular grid for a model containing the excitation box and its vicinity. During this step, the local structural model is inserted into the excitation box, and complete source-path-site effects are computed (see Figure 1). During the second step, the excitation box remains fully permeable for the scattered wavefield coming into and outside the excitation box. A similar approach for 3D finite-elements method was presented by Bielak et al. [2], Yoshimura et al. [3].

A replication test is performed to verify a correct connection between the first and second steps. To that goal, the second step is performed without any change of the structure with respect to the first step. In this case the computed complete wavefield inside the excitation box should be the same as that computed in the first step, while the scattered wavefield outside the box should be zero.

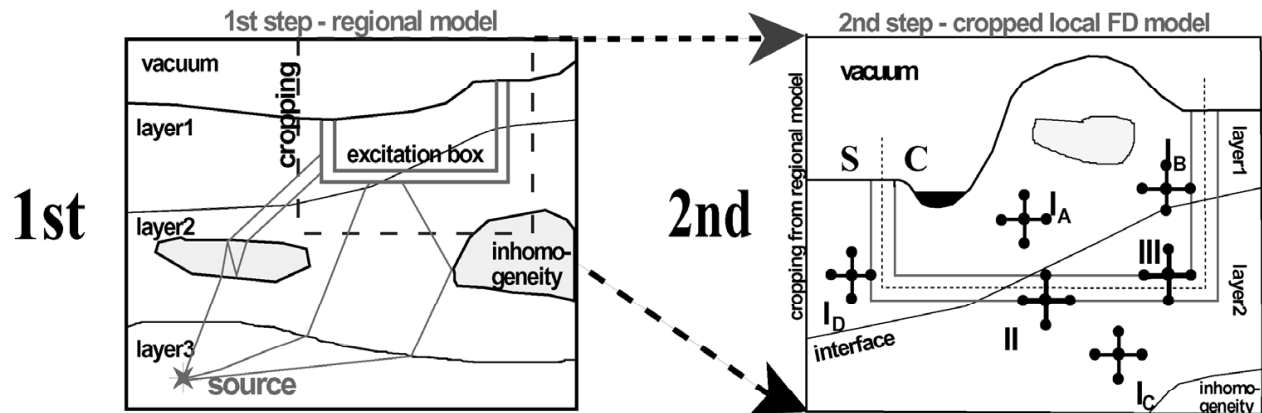


Figure 1: The principle of the two-step hybrid method. The 1<sup>st</sup> step of the approach (left) is computed on a large simple structural model. The time history of wavefield on a formal excitation box is saved on disk. The 2<sup>nd</sup> step model (right) is performed on a fraction of the original model. A new local structure is inserted inside the excitation box. This box formally divides the computational domain into C and S parts, where the complete ( $U_C$ ) and scattered ( $U_S$ ) wavefields are computed, respectively.

### Finite-extent source – 1<sup>st</sup> hybrid step

The  $M_w=5.9$  Athens earthquake source and path effects considered in the 1<sup>st</sup> step of this method are, in this paper, computed by the PEXT method (Zahradník and Tselentis [4]). PEXT method models finite-extent source complexities by stochastic PERTurbation and EXtrapolation of the deterministic wavefield (Figure 2). The low-frequency part contains the near, intermediate and far-field source terms, as well as the effects of the free surface and 1D crustal structure. In contrast to the referenced paper, all perturbation

and extrapolation is applied only for the high-frequency part. The low-frequency part remains unchanged, without any perturbation here.

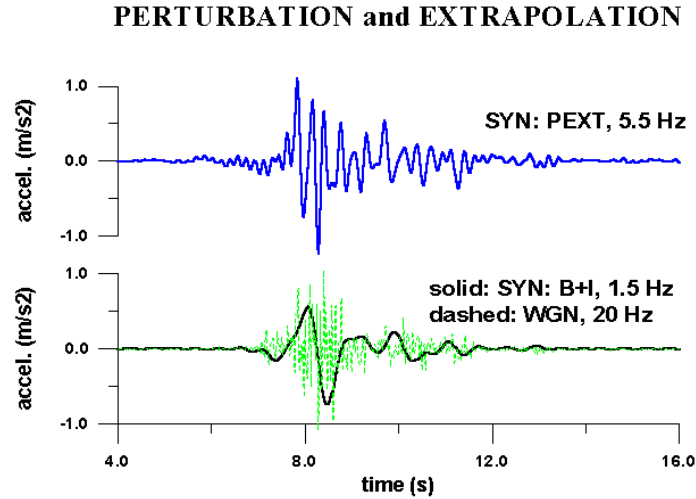


Figure 2: Explanation of the PEXT method (using other numerical parameters than in this paper). Bottom panel: B+I Bouchon's [6] point source summation with Irikura's [5] enhancement trick, all up to 1.5 Hz only, used to construct the shaping window, and the Gaussian noise (up to 20 Hz) shaped by that window. Top panel: PEXT method up to 5.5 Hz, comprising the perturbation and extrapolation of the B+I synthetics, and the stochastic component from the bottom panel (from Zahradník and Tselentis [4]).

Composite-source modeling is based on calculation of the point-source synthetics for a set of relatively few (equally sized) subevents. Their moment rate is expressed by Brune's causal time function. The subevents are subjected to the EGF-like summation, including the low-frequency artificial enhancement (Irikura and Kamae [5]). In this paper, the deterministic calculation and summation are made up to (and slightly beyond) the corner frequency of the subevent, where the summation is incoherent, hence the source poses realistic directivity. After that, a shaping window is derived from these low-frequency acceleration time series. Finally, Gaussian noise is generated, having flat acceleration spectrum (omega-squared model), and it is shaped by the time window derived before. In this way, the phase of the stochastic high-frequency radiation is defined. The amplitude of the stochastic high-frequency radiation is kept the same as that of the deterministic spectral plateau, unless the attenuation correction (kappa effect) is employed. The method uses complete Green's functions computed by the DWN (Bouchon [6]; Coutant [7]). The model of this paper has the following parameters: length and width  $L = 10$  km,  $W = 8$  km (corresponding to Somerville et al. [8]), source composed of  $5 \times 5 = 25$  subevents, each subevent with the slip duration ( $= 1/\text{corner frequency}$ ) = 0.57 sec, and average slip = 0.059 m.

The Athens fault length estimated from low-frequency information was of about 15 km, that from high-frequency information was considerably smaller. The latter was supported by early aftershocks as shown in Figure 3. Therefore, we consider a single asperity 4.0 km x 4.8 km, with slip contrast = 2.2. The nucleation point is assumed to be at 38.08 N, 23.58 E - the westernmost part of the model - at the depth of 10 km, at the bottom corner of the asperity. For the rest of the rupture area, a homogeneous slip is set to maintain the moment. Upper edge of the fault plane is at 8 km depth. Rupture propagates radially with velocity = 2.8 km/s, with a 10% perturbation of the rupture time. The average slip velocity on asperity is  $0.059 \times 2.2 / 0.57$  m/s = 0.23 m/s. The maximum slip velocity depends on the wavelet used, and, in the case of Brune's wavelet it is (average slip velocity \* 2.3) = 0.24 m/s. The deterministic modeling is made up to 2.8 Hz, and the resulting acceleration spectral plateau (averaged between 2.0 and 2.8 Hz) is

stochastically extrapolated up to 6 Hz, as described above. Attenuation effect is included via  $\kappa=0.05$  s.

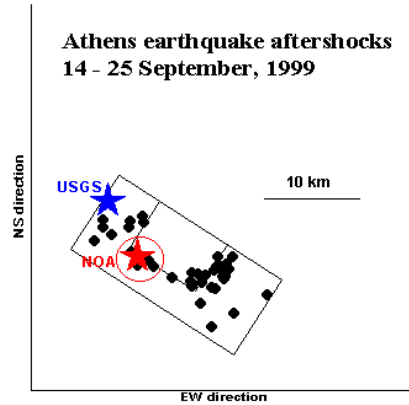


Figure 3: The plane view of September 14 - 25, 1999 aftershocks (full circles) and the two fault extents considered in the first stages of the study: The outer rectangle (in-fault size 20 km x 16 km), and the inner one (10 km x 8 km). The USGS-NEIC epicenter is compared with the epicenter re-located by NOA (National Observatory of Athens, Papadopoulos et al. [9]). From Tselentis and Zahradník [10].

The source model was verified against the strong-motion acceleration waveforms recorded in the central part of Athens (Kalogeras and Stavrakakis [11]; Ambraseys et al. [12]), see Figure 4. The dominant frequencies of velocities were of about 0.6 Hz.

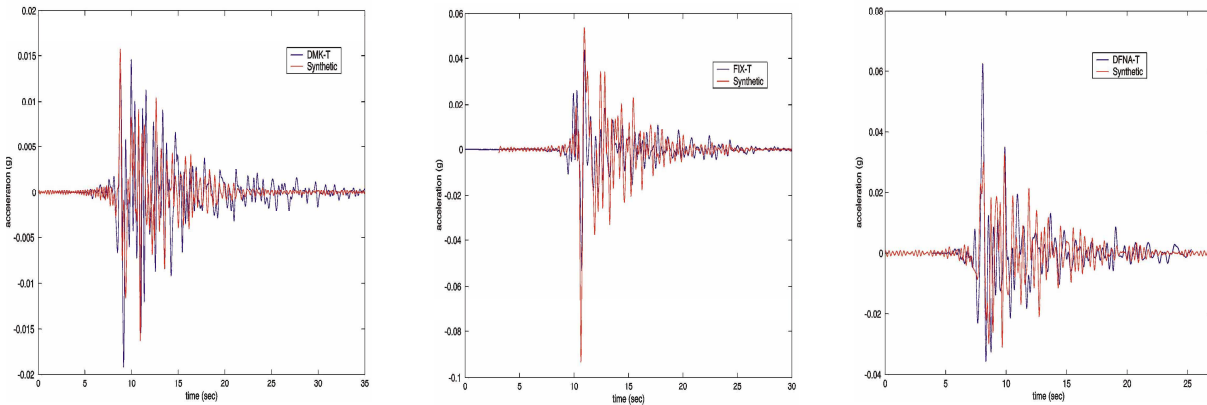


Figure 4: The comparison of the PEXT synthetics with strong motion data verifying the source model.

### 3D finite-difference method – 2<sup>nd</sup> hybrid step

3D FD method (Opršal and Zahradník [1], Opršal et al. [13]) solves the elastodynamic partial differential equation (PDE) in the time domain for Hooke's isotropic generally inhomogeneous medium containing internal discontinuities and non-planar topography. The formulation is a 3D explicit FD approximation to the 2<sup>nd</sup> order hyperbolic PDE. The accuracy in homogeneous regions is of the 2<sup>nd</sup> order in space and time. The FD formulation is stable for high  $V_P / V_S$  ratios but, due to free-surface accuracy limitation, it is better to avoid cases of  $V_P / V_S > 4$ . The heterogeneous formulation uses single formula everywhere, and the traction continuity is implicitly approximated via proper treatment of the discontinuous elastic

parameters. Same formula is applied also at the free surface above which the parameters are zeroed (vacuum formalism). The FD method performs on spatially irregular rectangular grids. It is an extension of 2D P-SV case of Opršal and Zahradník [14].

The irregular grid not only avoids over-sampling of high-velocity regions, but the grid refinement also reduces the stair-case free-surface artifacts. The irregular grid is defined by three independent 1D vectors. Transparent boundaries (Emerman and Stephen [15]) and damping tapers (Cerjan [16]) at the edges of the model are used.

## ANO LIOSIA SITE EFFECTS

### Motivation

The main motivation to focus this study just on the Ano Liosia area, a NW suburb of Athens, were intensities as high as IX observed at this site during the 1999 earthquake. Another reason was an extremely pronounced H / V ratio ( $H / V = 4.4$ , see Figure 5) found for this site from aftershock measurements (and also from noise measurements) performed in an extended area around the epicentral region. The measurements were done at a 30-station temporary network installed in Athens after the mainshock by the Seismological Laboratory, the University of Patras (Tselentis and Zahradník [17]). Both the intensities and H/V ratios indicated that Ano Liosia is a "singular" site.

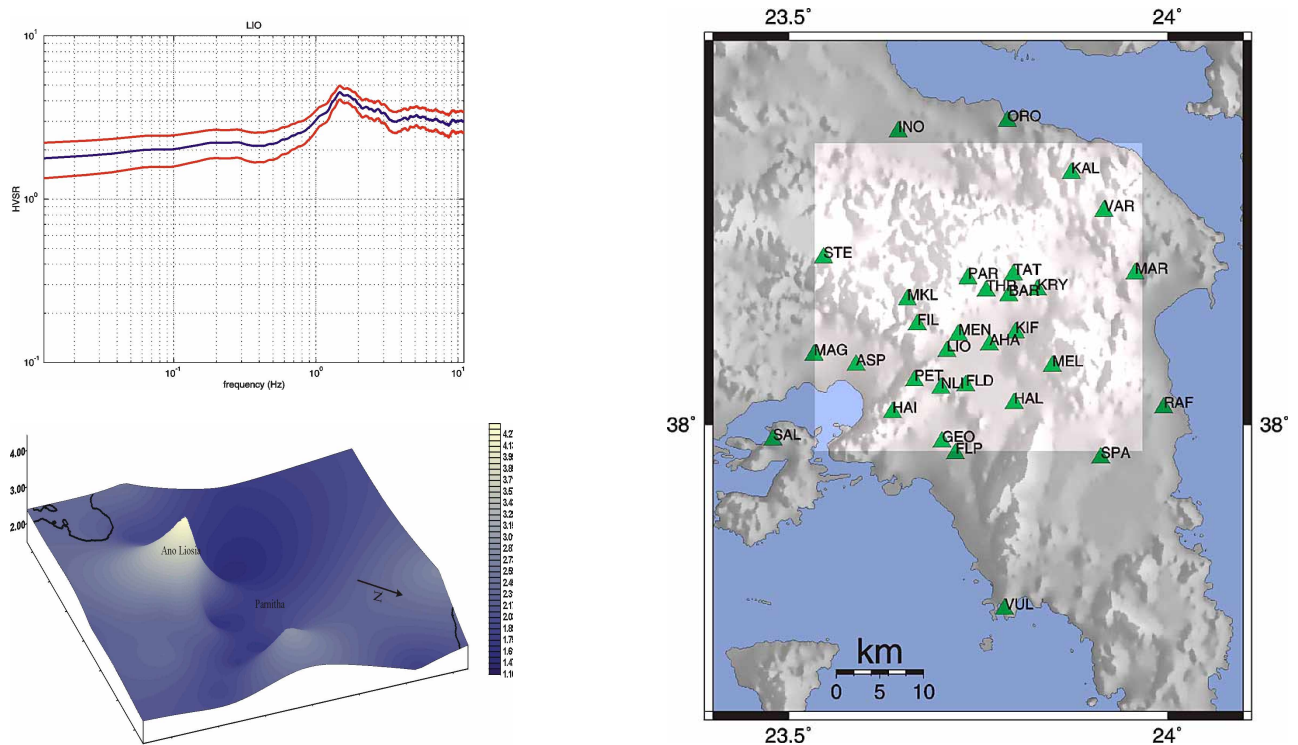


Figure 5: "Singularity" of the Ano Liosia area. The left upper panel shows frequency dependence of H / V ratios at Ano Liosia measured from the aftershocks, the blue line is the averaged value, the red lines are the uncertainty bounds. The left lower panel depicts the maxima of the H / V ratios measured for the aftershocks in the whole studied region close to Athens (highlighted rectangle at the right panel).

### Source-site situation and geology

The fault model, the most heavily damaged sites of Athens (including Ano Liosia), and the FD excitation-box are depicted in Figure 6.

# Ano Liosia area

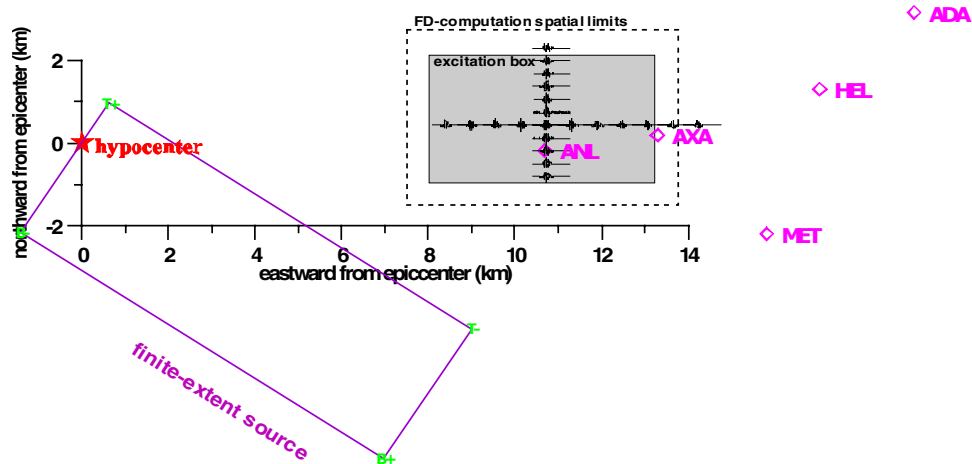


Figure 6: The plane view of the source-site configuration studied in this paper. The diamonds are the Athens suburbs with intensity IX, including Ano Liosia = ANL. Red star is epicenter situated on the edge of the finite-extent source (represented by the violet rectangle). The FD computational area and excitation box (highlighted) include two profiles showing synthetic accelerograms of the background wavefield (the peak was about 0.2g).

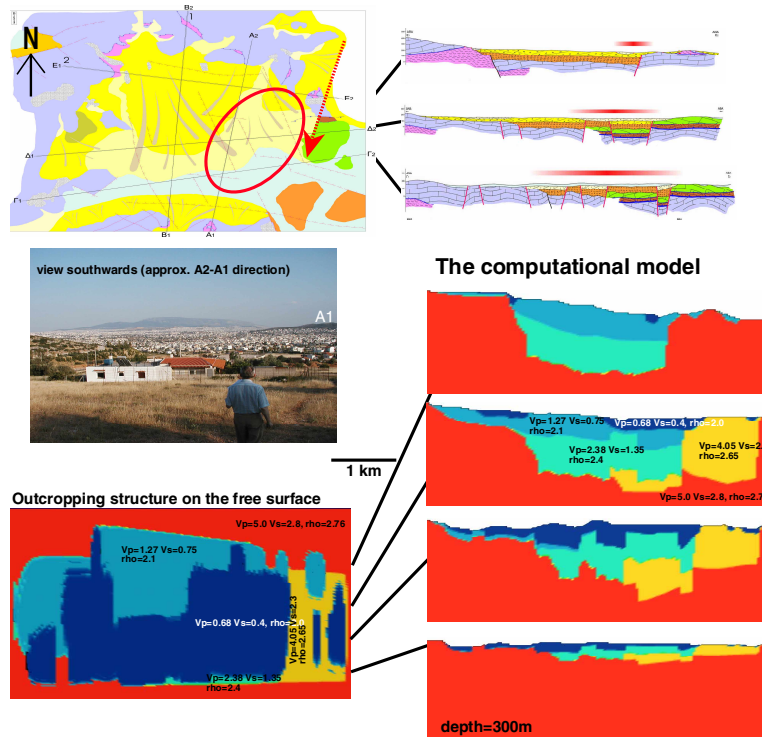


Figure 7: The model of Ano Liosia area. The upper panels represent geological model; the surface structures are shown on the left, three vertical cross-sections along profiles E1-E2, D1-D2 and G1-G2 are specified on the right (Lekkas et al. [18]). The red ellipse is an approximate extent of the largest damages

observed after the mainshock. The red arrow shows the viewing direction to the densely populated area (see photo). The A1 on the photo corresponds to the A1 point in the upper left panel. The bottom left panel is the surface structure as it appears on the free surface of the computational model created by the interpolation of the three geological cross-sections in the NS direction. The bottom right quaternion are corresponding cross-sections of the computational model in the EW direction. An animation of these EW parameter slices as viewed when we move in the NS direction through the whole computational model is available on demand, or at WWW page referenced below. The shear velocity  $V_S$  ranges from 0.4 to 2.8 km/s.

The geological information about the Ano Liosia area is relatively sparse for this kind of investigation. In fact only three specified profiles were convenient for creating the model (see Figure 7). Two more profiles containing only 'bedrock' were added to at the edges of the model. The interfaces between blocks defined in these five profiles were linearly interpolated in the NS direction and a digital model was created. The model was used in the form of 3D function  $a = a(X)$ , where  $a$  is a parameter vector ( $a = (\lambda, \mu, \rho, Q_p, Q_s)$ ) for each position vector  $X = (x, y, z)$  and  $x, y, z$  are the coordinates in meters. For more details on definition of the 'geological', 'digital' and 'computational' model, see Opršal and Zahradník [1], section 2.5.

### **Combined source-path-site effects**

After computing the excitation due to the source and path effects by PEXT method, the 2<sup>nd</sup> step includes the site effects by means of the FD method. The synthetic velocigrams and accelerograms together with peak horizontal velocity and acceleration (frequency band 0.0-6.0Hz) are shown in Figure 8. The whole area show in Figures 8 and 9 is the surface part of the excitation box, thus the whole area shows complete wavefield of the hybrid computation.

The pseudo acceleration response (PSR) spectra are shown in Figure 9. The total horizontal component of the PSR was computed. We can also see the spatio-frequency distribution of the PSR maxima.

The wavefield clearly shows a pronounced amplification and prolongation, but its space and time pattern is very complicated, thus not enabling any simple interpretation in terms of a specific sediment type or a particular geometrical feature of the basin. The maximum velocities are just below 0.8 m/s, the maximum accelerations are  $8.5 \text{ m/s}^2$ , the maximum response spectra are  $43 \text{ m/s}^2$ . These values are relatively high, but the spots of such high values are isolated. They mainly correspond to the high velocity contrast ( $\sim 7$ ). The region with highest observed intensities (marked by the ellipse in Figure 7) shows a more realistic velocity and acceleration values of 0.5 m/s and  $5.5 \text{ m/s}^2$ , and PSR  $28 \text{ m/s}^2$ .

The peculiar image of the maximum amplitudes in Figures 8 and 9 calls for a continuing study with a more detailed structural model. Indeed, the present geological information is too sparse to be simply interpolated. Smoothing the model in the E-W direction (smoothing window of 75 m and 225 m) was helpful in general, but the maximum amplitudes even increased, because the domains of low velocities were larger than the smoothing window. On the other hand, a larger smoothing window would probably modify the model too much.

Animations of the horizontal-velocity wavefield are available at:

<http://geo.mff.cuni.cz/> -> people -> Ivo Oprsal

The codes are available upon request.

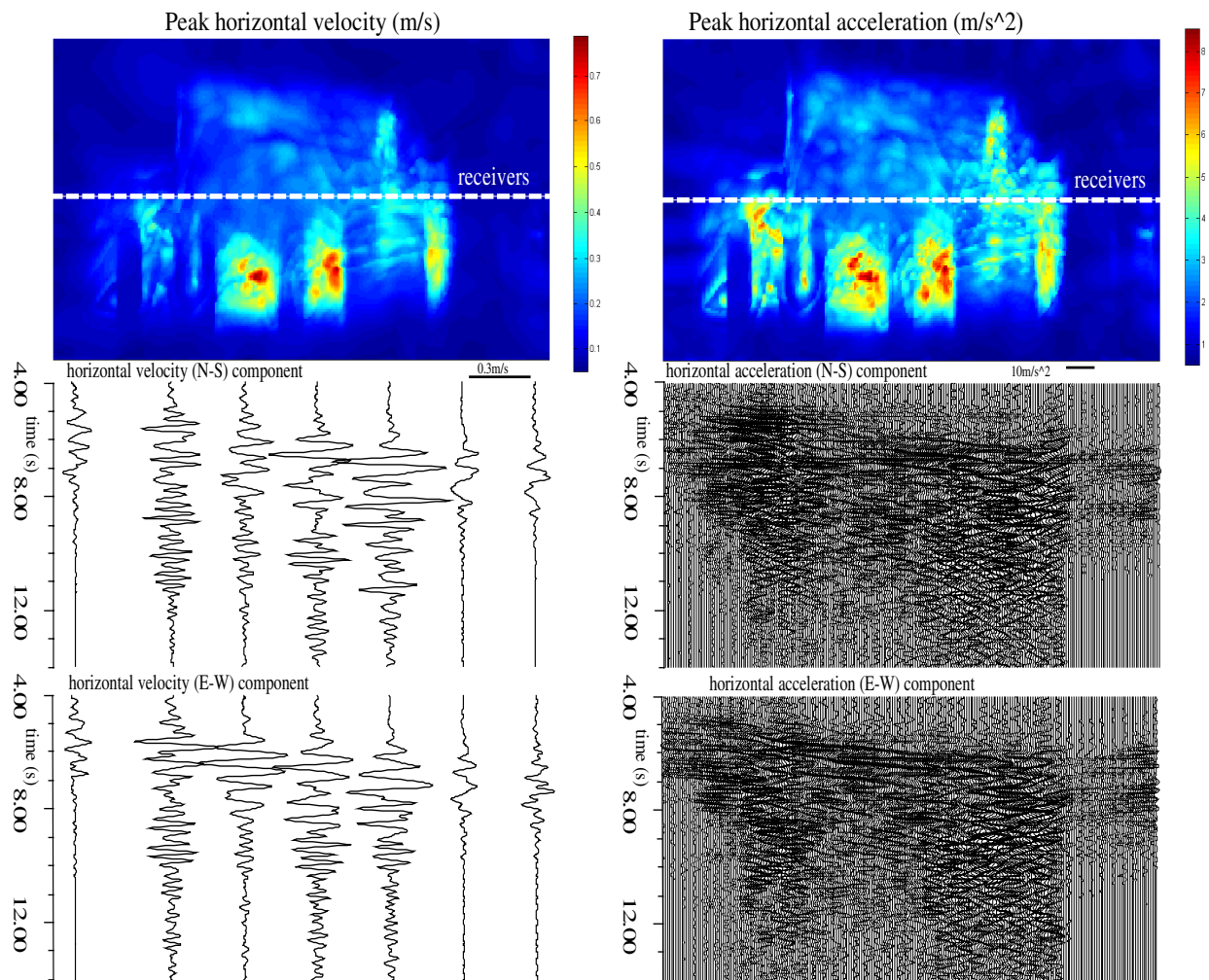


Figure 8: Resulting strong ground motions due to combined source, path and site effects for the 1999 Athens earthquake at the Ano Liosia region. Synthetic velocities (left panel) and accelerations (right panel) are shown here. The upper panels are the maximum reached total-horizontal-component values on the topographic free surface. The bottom panels are corresponding synthetics shown, for simplicity, just for a single line of receivers (the white dashed line of the upper panels). The investigated frequency band is 0.0 - 6.0 Hz. The area shown corresponds to the excitation box depicted by the grey rectangle in Figure 6. None of the receivers on the white dashed line is on bedrock except the two receivers on the left and right edges.

## Overall maxima of pseudo-acceleration response

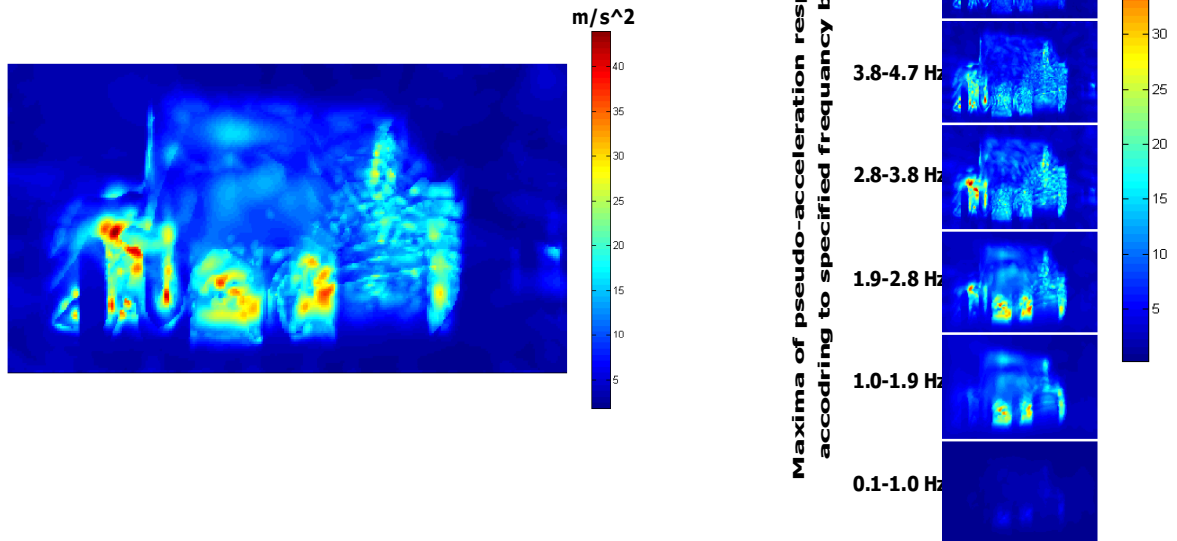


Figure 9: The pseudo-acceleration spectra for the Ano Liosia area - total horizontal component. The maximum reached values are shown (left panel), together with the spectral decomposition into 7 frequency bands (right panel). The damping is 5% of critical, and the overall frequency band is 0.0 - 6.0Hz. The shown area corresponds to the excitation box depicted by the grey rectangle in Figure 6.

## CONCLUSIONS

- 1) Hybrid approach allows *a very efficient* joint treatment of finite-extent source, path and site effects up to frequencies of the engineering interest (here up to 6 Hz).
- 2) The 3D input (bedrock) motion due to finite source was calculated by PEXT method, and validated by comparison of synthetic and observed strong motion (mainshock) records, available in the other sites in Athens.
- 3) Strong damage and intensity IX at Ano Liosia site proved to be a combined effect of proximity and directivity of the source, and complex 3D site effects.

## ACKNOWLEDGEMENTS

This research was supported by research project of Czech Republic MSM 113200004, Grant Agency of Czech Republic GACR 205/03/1047, GAUK grant 235/2003, and by project: 'Study on the master model for strong ground motion prediction toward earthquake disaster mitigation'; principal investigator: Kojiro Irikura, DPRI, Kyoto University. This is a contribution No. 1314 of the Geophysical Institute of ETH Zurich.

## REFERENCES

1. Opršal, I., Zahradník, J. "3D Finite Difference Method and Hybrid Modelling of Earthquake Ground Motion." JGR -Solid earth, 2002, 107, 10.1029/2000JB000082, 16 pp.

2. Bielak, J., Loukakis, K., Hisada, Y., Yoshimura, C. "Domain Reduction Method for Three-Dimensional Earthquake Modeling in Localized Regions, Part I: Theory." *Bull. Seismol. Soc. Am.*, 2003, 93, 817-824.
3. Yoshimura C., Bielak J., Hisada Y. and Fernandez A. "Domain Reduction Method for Three-Dimensional Earthquake Modeling in Localized Regions, Part II: Verification and Applications." *Bull. Seismol. Soc. Am.* , 2003, 93, 825-840.
4. Zahradník, J., and Tselentis, G.-A. "Modeling strong-motion accelerograms by PEXT method, application to the Athens 1999 earthquake." *Proc. of XXVIII Gen. Ass. of Europ. Seismol. Comm*, 1-6 Sep. 2002, Genoa (CD-ROM), or <http://seis30.karlov.mff.cuni.cz/>
5. Irikura, K., and K. Kamae "Estimation of strong motion in broad-frequency band based on a seismic source scaling model and an empirical Green's function technique." *Annali di Geofisica*, 1994, 37, 1721-1743.
6. Bouchon, M. "A simple method to calculate Green's functions for elastic layered media." *Bull. Seismol. Soc. Am.*, 1981, 71, 959-971.
7. Coutant, O., "Programme de simulation numerique AXITRA." Rapport LGIT, 1989, Universite Joseph Fourier, Grenoble.
8. Somerville, P., K. Irikura, R. Graves, S. Sawada, D. Wald, N. Abrahamson, Y. Iwasaki, T. Kagawa, N. Smith, A. Kowada "Characterizing crustal earthquake slip models for the prediction of strong ground motion." *Seism. Res. Lett.* , 1999, 70, 59-80.
9. Papadopoulos, G. A., Drakatos, G., Papanastassiou, D., Kalogeras, I., and G. Stavrakakis "Preliminary results about the catastrophic earthquake of 7 September 1999 in Athens, Greece." *Seism. Res. Lett.*, 2000, 71, 318 -329.
10. Tselentis, G.-A., Zahradník, J. "The Athens earthquake of September 7, 1999." *Bull. Seism. Soc. Am.*, 2000, 90, 1143-1160.
11. Kalogeras, I., Stavrakakis, G. "Processing of the strong-motion data from the September 7<sup>th</sup>, 1999 Athens earthquake." Geodynamic Institute, National Observatory of Athens, 1999.
12. Ambraseys, N., Smit, P., Berardi, R., Rinaldis, D., Cotton, F., C. Berge-Thierry "Dissemination of European Strong-Motion Data." CD-ROM collection, 2000. European Council, Environment and Climate Research Programme.
13. Opršal, I., Brokešová, J., Fäh, D., Giardini, D. "3D Hybrid Ray-FD and DWN-FD Seismic Modeling For Simple Models Containing Complex Local Structures." *Stud. Geophys. Geod.*, 2002., 46, 711-730.
14. Opršal, I., Zahradník, J. "Elastic finite-difference method for irregular grids." *Geophysics*, 1999, 64, 240-250.
15. Emerman, S., H., Stephen, R., A. "Comment on 'Absorbing Boundary Conditions for Acoustic and Elastic wave Equations' " by R. Clayton and B. Enquist. *Bull. seismol. Soc. Am.*, 1983, 73, 661-665.
16. Cerjan C., Kosloff, R., Reshef, M. "A nonreflecting boundary condition for discrete acoustic and elastic wave equations." *Geophysics*, 1985, 50, 705-708.
17. Tselentis, G.-A., Zahradník, J. "Aftershock monitoring of the Athens earthquake of September 7, 1999." *Seism. Res. Letters*, 2000, 71, 330-337.
18. Lekkas, E., Lozios, S., G., Danamos, G., D., Soukis, K., Vasilakis, E. "Microzonation Study of Ano Liosia." Report of 'Program of Seismic Protection, Municipality of Ano Liosia. Microzonation Study' (in Greek), 2000.